Measurement-induced quantum fluctuations and bistability of a relativistic electron in a Penning trap

M. Rigo,[1] G. Alber,[2] F. Mota-Furtado,[1] and P. F. O'Mahony[1]
[1]*Department of Mathematics, Royal Holloway, University of London, Egham, Surrey TW20 OEX, United Kingdom*
[2]*Abteilung für Quantenphysik, Universität Ulm, D-89069 Ulm, Germany*
(Received 14 January 1998)

A detailed quantum-mechanical description of an electron in a Penning trap is developed in which nonlinear relativistic effects as well as stochastic effects arising from radiative damping and the continuous measurement of the electronic motion are taken into account. A master equation is derived that describes the influence of these environmental effects on the bistable dynamics of the electron. Manifestations of measurement-induced fluctuations on the bistable dynamics of individual continuous measurement processes are investigated with the help of the quantum state diffusion model. [S1050-2947(98)04807-0]

PACS number(s): 32.80.Pj, 03.65.Bz, 42.50.Lc, 05.30.Ch

I. INTRODUCTION

The advances in trapping and cooling techniques within the past decade have led to new experiments that can continuously observe individual quantum systems by optical or electronic means. One of the most elementary quantum systems that has been investigated in this context is an electron in a Penning trap [1]. A spectacular application of its experimental realization has been the measurement of the electronic g-factor with unprecedented accuracy. However, besides applications in quantum metrology, this elementary quantum system also offers new possibilities for fundamental studies on the influence of continuous quantum measurement processes on the electronic dynamics.

In a series of recent experiments, Gabrielse and coworkers have investigated the nonlinear effects that are caused by the relativistic motion of an electron in a Penning trap [2–4]. Based on purely classical considerations, the existence of such nonlinear effects due to relativistic corrections has been predicted theoretically by Kaplan [5]. Typically in these experiments the electronic dynamics is monitored by purely electronic means by detecting the currents that are induced by the axial motion of the electron in the end-caps of the electrodes. The axial motion of the trapped electron is coupled to its spin and cyclotron degrees of freedom by relativistic effects. Thus the continuous observation of the axial electronic motion through monitoring the charge-induced currents also yields information about the dynamics of the electronic spin and cyclotron motion.

A number of recent theoretical studies have considered the relativistic dynamics of an electron in a Penning trap. For instance, in [6] this system is suggested as an experimental realization of a quantum nondemolition measurement of the cyclotron excitation number of the electron. This work appropriately introduces the dissipation in the axial motion by using the theory of open quantum systems but assumes that the cyclotron state is projected onto a Fock state without describing how this collapse occurs. Furthermore, it neglects other dissipative effects, thus limiting its applicability to a short time scale, which is impractical for typical experimental investigations. In [7] a model of electron dynamics involving cyclotron and axial dissipation is introduced together with a phase sensitive measurement involving the squeezing of the bath. The measurement-induced influence on the cyclotron motion is investigated by eliminating the axial motion adiabatically. It is found that the bistable nonlinear resonance can be modified by varying one of the squeezing parameters associated with the phase sensitive detection process. However, all these investigations are based on simplified model systems in which either the dissipative effects or the relativistic dynamics of the electronic degrees of freedom that are relevant for typical experiments are not fully taken into account.

Motivated by the recently performed experiments of Gabrielse *et al.* [2–4], in the following a detailed quantum-mechanical description of the relativistic electronic dynamics in a Penning trap is developed. Thereby the main emphasis is put on a realistic and consistent quantum-mechanical treatment of the measurement-induced quantum fluctuations on the relativistically induced hysteresis effects. A master equation is derived in which all relativistic effects as well as all dissipative effects, which are dominated by radiative damping of the cyclotron motion and the continuous quantum measurement process, are taken into account. In order to obtain insight into the resulting time evolution of individual quantum measurement records, this master equation is simulated stochastically with the help of the quantum state diffusion model [8,9].

In Sec. II we develop a detailed theoretical description of an electron in a Penning trap taking into account relativistic corrections as well as external, electric driving fields and all the dominant environmental effects. A simplified master equation is derived for the experimentally interesting case of large axial driving and damping in which the axial motion can be eliminated adiabatically. Starting from this master equation, the spin and cyclotron motions are investigated in Secs. III and IV. Insight into the time evolution of individual continuous quantum measurement processes is obtained with the help of the quantum state diffusion model. Section III focuses on the question as to how relativistic effects influence the electronic spin motion. In Sec. IV the back action of the continuous measurement process on the bistable dynamics of the electronic cyclotron motion is investigated. It is

demonstrated that the measurement-induced quantum fluctuations may influence these hysteresis effects significantly.

II. THEORETICAL FRAMEWORK

We develop in this section a theoretical description of the relativistic dynamics of an electron in a Penning trap. Starting from the Dirac Hamiltonian in Sec. II A the dominant relativistic corrections are discussed that lead to anharmonic, nonlinear terms in the Hamiltonian. In Sec. II B it is demonstrated that resonant driving of the electron by a periodic, external electric field may lead to bistable behavior. Radiative damping and the continuous measurement of the axial electronic motion are the dominant environmental influences. Together with the relativistic Hamiltonian, they determine the master equation of the trapped electron, which is presented in Sec. II C. In Sec. II D the axial electronic motion is eliminated adiabatically in the limit of large driving and damping of the axial motion. Thus a simplified description of the spin and cyclotron degrees of freedom is obtained. This master equation might be used as a starting point for stochastic simulations of individual measurement records. Basic facts about stochastic simulations are discussed in Sec. II E with the help of the quantum state diffusion model.

A. The relativistic Hamiltonian of an electron in a Penning trap

The relativistic Dirac Hamiltonian of a spin-half electron under the influence of an external electromagnetic field can be reduced to its nonrelativistic limit with the help of the Foldy-Wouthuysen transformation [10]. In the case of an electron in a Penning trap, the relevant magnetic field $\mathbf{B}$ is time independent and the electric field $\mathbf{E}$ divergence free, thus the relativistic corrections (RC) can be further simplified yielding the Hamiltonian $H_0=H_{\mathrm{NR}}+H_{\mathrm{RC}}$. The nonrelativistic (NR) part of this Hamiltonian is determined by

$$H_{\mathrm{NR}}=\frac{\boldsymbol{\pi}^2}{2m}+e\Phi-\frac{g\mu_B}{2}\,\boldsymbol{\sigma}\cdot\mathbf{B} \tag{1}$$

and the relativistic corrections are given by

$$H_{\mathrm{RC}}=-\frac{(\boldsymbol{\pi}^2-2m\mu_B\boldsymbol{\sigma}\cdot\mathbf{B})^2}{8m^3c^2}-(1+2a)\,\frac{\mu_B}{2mc^2}\,\boldsymbol{\sigma}\cdot\mathbf{E}\times\boldsymbol{\pi}$$
$$+\frac{a\mu_B}{2m^2c^2}\,\boldsymbol{\sigma}\cdot\boldsymbol{\pi}\mathbf{B}\cdot\boldsymbol{\pi}. \tag{2}$$

Thereby terms up to the order of $(1/c^2)$ have been taken into account. The electron rest mass is denoted m and e and g are the electronic charge and g-factor with its associated anomaly $a=(g-2)/2$. The Bohr magnetron is given by $\mu_B=e\hbar/2m$ and $\boldsymbol{\sigma}$ and $\boldsymbol{\pi}=\mathbf{p}-e\mathbf{A}$ are the Pauli spin vector and the kinetic momentum operator, respectively. The rest energy mc^2 has been neglected in the Hamiltonian H_{RC}.

An electron in a Penning trap is subjected to a spatially uniform magnetic field $\mathbf{B}=B_0\mathbf{e}_z$ directed along the trap axis and a quadrupole electrostatic potential Φ [1]. This latter potential and the vector potential $\mathbf{A}_0$ associated with the magnetic field, expressed in the Coulomb gauge, are given by

$$\mathbf{A}_0=\frac{1}{2}B_0(-y\mathbf{e}_x+x\mathbf{e}_y),\quad \Phi=\frac{\Phi_0}{4d^2}(2z^2-x^2-y^2), \tag{3}$$

where d characterizes the spatial extension of the trap.

If a classical nonrelativistic particle is subjected to a magnetic field, it will evolve along a circular cyclotron orbit with frequency $\omega_c=eB_0/m$. In order to confine also the axial motion of the electron, an electrostatic quadrupole potential is superimposed onto the magnetic field. As a consequence, the motion of the particle can be decomposed into an axial harmonic motion of frequency $\omega_z^2=e\Phi_0/md^2$ and a planar motion itself composed of the fast harmonic cyclotron motion at the modified frequency $\omega_+=\omega_c-\omega_-$ and the much slower circular magnetron motion with frequency $\omega_-=\omega_z^2/2\omega_+$. For an electron in a Penning trap these characteristic frequencies typically differ in scale by three orders of magnitude, i.e., $\omega_-\ll\omega_z\ll\omega_+$.

In the quantum case, the particle's motion is decomposed into normal modes in an analogous way. For this purpose, creation (annihilation) operators $a_z^\dagger$ (a_z), $a_+^\dagger$ (a_+), and $a_-^\dagger$ (a_-) are introduced for the axial, cyclotron, and magnetron motion [11] to transform the Hamiltonian H_0 into normal coordinates. Introducing the spin precession frequency $\omega_s=\frac{1}{2}g\omega_c$, the nonrelativistic part of the Hamiltonian can be written in the familiar form [1]

$$H_{\mathrm{NR}}=\hbar\omega_+a_+^\dagger a_++\hbar\omega_za_z^\dagger a_z-\hbar\omega_-a_-^\dagger a_-+\frac{1}{2}\hbar\omega_s\sigma_z. \tag{4}$$

Under typical experimental conditions the magnetron motion is metastable with a damping time of the order of years so that it does not produce a relevant instability.

In the normal mode representation of the relativistic Hamiltonian H_{RC} use can be made of the previously mentioned hierarchy of characteristic frequencies to perform an adiabatic approximation. A simplified Hamiltonian that describes properly the dynamics on time scales large compared to the slowest characteristic time scale in a Penning trap, namely the magnetron time scale $(2\pi)/\omega_-$, is obtained by neglecting all the terms that oscillate rapidly in time relative to the magnetron time scale as well as all the negligibly small contributions of order (ω_-/ω_+) and $(\omega_z/\omega_+)^2$. Thus H_{RC} reduces to [12]

$$H_{\mathrm{RC}}\cong-\frac{\hbar^2\omega_+^2}{2mc^2}\left(1+\frac{\omega_z}{2\omega_+}+\frac{\omega_c}{\omega_+}\sigma_z+a_+^\dagger a_+\right)$$
$$\times a_+^\dagger a_+-\frac{\hbar^2\omega_+\omega_c}{4mc^2}\left(1+\frac{g\omega_z}{4\omega_+}\right)\sigma_z-\frac{\hbar^2\omega_+\omega_z}{2mc^2}$$
$$\times\left(\frac{1}{2}+\frac{g}{4}\,\frac{\omega_c}{\omega_+}\sigma_z+a_+^\dagger a_+\right)a_z^\dagger a_z. \tag{5}$$

Equation (5) describes the relativistic corrections that are of central interest in the present work, namely, shifts of the trap-eigenfrequencies and nonlinear couplings between the cyclotron, axial, and spin motions. A dynamical consequence of the Hamiltonian in Eq. (5) is the appearance of a bistable domain with its associated hysteresis effect in the case of resonant excitation by external electromagnetic fields. Fur-

thermore, the nonlinear couplings between the different motions is an important effect that is exploited for the continuous measurement of the electronic cyclotron and spin motion.

B. The influence of periodic, external electric fields

In order to monitor the bistable dynamics of an electron in a Penning trap, typically two additional periodic electric fields are applied. The first of these two fields is a sinusoidal voltage applied between the ring electrode and one end-cap of the Penning trap [3]. It is oscillating at a frequency ω_d almost resonant with the axial frequency of motion $\omega_d \simeq \omega_z$. The associated vector potential $\mathbf{A}_1$ can be expressed in terms of the amplitude U_0 of this voltage and the minimal distance $2z_0$ between the end-caps, namely,

$$\mathbf{A}_1 = \frac{U_0}{2z_0\omega_d}\cos(\omega_d t)\mathbf{e}_z . \tag{6}$$

The second applied electric field is typically polarized in the cyclotron-magnetron plane, and its frequency ω_p is tuned close to the cyclotron frequency $\omega_p \simeq \omega_+$. Such a field can be applied, for instance, by sending a microwave electric field through an opening in the Penning trap [2,3]. This planar driving field can be represented by the vector potential

$$\mathbf{A}_2 = -\frac{i}{\omega_p}(\mathbf{E}_0 e^{-i\omega_p t} - \mathbf{E}_0^* e^{i\omega_p t}), \tag{7}$$

where $\mathbf{E}_0$ is the amplitude of the electric field polarized in the x-y plane. Thus according to Eqs. (3), (6), and (7) the total vector potential acting on the electron in a Penning trap is given by $\mathbf{A} = \mathbf{A}_0 + \mathbf{A}_1 + \mathbf{A}_2$. Introducing the new potential vector into the Hamiltonian H_0 and performing the normal mode decomposition and adiabatic approximation as described above gives the Hamiltonian term (5) plus an extra contribution H_{driving} that describes the effects originating from the driving fields. This latter contribution can be further simplified with the help of the rotating wave approximation (RWA), thus yielding

$$\begin{aligned} H_{\text{driving}} = {} & \hbar(\beta a_+^\dagger e^{-i\omega_p t} + \beta^* a_+ e^{i\omega_p t}) \\ & + \hbar(\beta_z a_z^\dagger e^{-i\omega_d t} + \beta_z^* a_z e^{i\omega_d t}). \end{aligned} \tag{8}$$

The frequencies

$$\beta = -\frac{eE_0}{2\sqrt{2\hbar m\omega_+}} \quad \text{and} \quad \beta_z = -i\frac{eU_0}{4z_0\sqrt{2\hbar m\omega_z}} \tag{9}$$

describe the amplitudes of the planar and axial driving fields, respectively.

The frequency ω_d of the axial driving is almost in resonance with the axial frequency of motion, whereas it is largely detuned from the cyclotron and magnetron frequencies. This implies that within the framework of the RWA approximation, its effect on the cyclotron and magnetron motions is negligible. Therefore, the corresponding contributions have been omitted in Eq. (8). The same argument applies for the planar driving, which will have a noticeable influence only on the cyclotron motion. As a consequence, the magnetron operators do not contribute as they are oscillating with a frequency that is smaller by a factor of the order of (ω_-/ω_+). The magnetron motion is a simple harmonic motion at frequency ω_-, which is decoupled from all the other motions so it will no longer be considered explicitly in the subsequent treatment. Thus the Hamiltonian, which describes the relativistic electronic cyclotron, axial, and spin dynamics in the trap in the adiabatic approximation, is finally given by

$$\begin{aligned} H = {} & \hbar\Omega_+ a_+^\dagger a_+ + \hbar\Omega_z a_z^\dagger a_z + \frac{1}{2}\hbar\Omega_s\sigma_z - \hbar\omega_{\text{rc}} N a_z^\dagger a_z \\ & - \hbar\omega_{\text{rc}}\left(\frac{\omega_+}{\omega_z}\right)(1 + a_+^\dagger a_+ + \sigma_z)a_+^\dagger a_+ \\ & + \hbar(\beta a_+^\dagger e^{-i\omega_p t} + \beta^* a_+ e^{i\omega_p t}) \\ & + \hbar(\beta_z a_z^\dagger e^{-i\omega_d t} + \beta_z^* a_z e^{i\omega_d t}). \end{aligned} \tag{10}$$

In this expression, the first three terms represent the harmonic motions with the renormalized trap frequencies $\Omega_+ = \omega_+ - \omega_{\text{rc}}/2$, $\Omega_z = \omega_z - \omega_{\text{rc}}/2$, and $\Omega_s = \omega_c - g\omega_{\text{rc}}/4$. The frequency

$$\omega_{\text{rc}} = \frac{\hbar\omega_z\omega_+}{2mc^2} \tag{11}$$

characterizes the strength of the relativistic effects. The second line describes the nonlinear couplings induced by the relativistic effects. Here we have introduced the cyclotron and spin number operator

$$N = a_+^\dagger a_+ + \frac{g}{4}\sigma_z \tag{12}$$

and we have taken ω_c to be equal to ω_+ as they differ only by a factor of the order of $(\omega_z/\omega_+)^2$.

C. Environmental effects and master equation for the relativistic electron

The dominant interactions of the electron with its environment are the radiative coupling of the cyclotron motion to the thermal radiation field and the coupling of its axial motion to the resistor of the electric circuit involving the external driving voltage with amplitude U_0 [1,11]. The couplings to these environments can be treated in the Born-Markov approximation so that the reduced density operator of the electron in the Penning trap $\rho(t)$ obeys a master equation of the canonical Lindblad form

$$\dot{\rho} = -\frac{i}{\hbar}[H,\rho] + \sum_j \left(L_j\rho L_j^\dagger - \frac{1}{2}L_j^\dagger L_j\rho - \frac{1}{2}\rho L_j^\dagger L_j\right). \tag{13}$$

Thus, the deterministic part of the electronic dynamics is characterized by the Hamiltonian H of Eq. (10) and the stochastic part is described by environment operators L_j.

Due to the hierarchy $\omega_+ \gg \omega_z \gg \omega_-$ the coupling of the cyclotron motion to the thermal radiation field is most dominant [1]. Its radiative damping can be described by the two Lindblad operators [13,14]

$$L_1=\sqrt{(\overline{n}+1)\kappa}a_+ \quad \text{and} \quad L_2=\sqrt{\overline{n}\kappa}a_+^\dagger \tag{14}$$

with the spontaneous decay rate of the cyclotron motion $\kappa=e^2\omega_+^2/3\pi\varepsilon_0 mc^3$ and $\overline{n}=[e^{\hbar\Omega_+/k_BT}-1]^{-1}$ denoting the mean number of quanta of the thermal radiation field at temperature T.

In typical experiments, the axial electronic motion is monitored continuously by measuring the out-of-phase component of the current, which is produced by applying a sinusoidal driving voltage between the ring electrode and one of the end-caps of the trap. The influence of this external applied voltage on the axial motion can be modeled by a quantum mechanical L-C-R circuit [1,11]. Thereby the inductance $L_{\rm ind}$ and the capacitance C are related to the axial eigenfrequency ω_z by $\omega_z^2=1/(L_{\rm ind}C)$. In the quantum-mechanical description of this L-C-R circuit the charge operator Q and the current operator I are related to the destruction and creation operators a_z and $a_z^\dagger$ by [11,14]

$$Q=\sqrt{\frac{\hbar}{2\omega_z L_{\rm ind}}}\,(a_z+a_z^\dagger),$$

$$I=i\sqrt{\frac{\hbar\omega_z}{2L_{\rm ind}}}\,(a_z^\dagger-a_z). \tag{15}$$

The operator measured in typical experiments is the slowly varying component of the out-of-phase component of the current, i.e. [11],

$$I_{\rm out}=2\sqrt{\frac{\hbar\omega_z}{2L_{\rm ind}}}\,{\rm Im}(a_z e^{i\omega_d t}). \tag{16}$$

In the context of quantum optics this continuous measurement would correspond formally to a heterodyning detection of a photocurrent [15], provided one identified a_z with the destruction operator of a photon in a particular mode of the electromagnetic field.

In the rotating wave approximation the dissipative influence of the resistance R on the electronic axial motion can be described by the Lindblad operators [14,11]

$$L_3=\sqrt{(\overline{n_z}+1)\kappa_z}a_z \quad \text{and} \quad L_4=\sqrt{\overline{n_z}\kappa_z}a_z^\dagger \tag{17}$$

with the damping rate

$$\kappa_z=\frac{R}{L_{\rm ind}}. \tag{18}$$

The thermal influence of the resistor that is at temperature T_R is characterized by the mean thermal quantum number

$$\overline{n}=[e^{\hbar\omega_z/k_BT_R}-1]^{-1}. \tag{19}$$

The master equation (13) for the reduced density operator ρ, together with the Hamiltonian (10) and the Lindblad operators (14) and (17), is a main result of this section. It describes the dynamics of the electron in a Penning trap including the relativistic corrections and the dominant environmental effects.

D. Master equation for the spin and cyclotron motion

In order to improve the signal-to-noise ratio, in typical experiments the resistance R is made as large as possible [1]. As a consequence, the axial motion is strongly damped. This property can be used to simplify further the master equation (13) by eliminating the axial motion adiabatically. This adiabatic elimination has already been described in detail for a nonrelativistic electron in a Penning trap [11] and can be applied to the master equation (13) in an analogous way. Thus the subsequent discussion focuses only on the general ideas of this elimination procedure.

When the damping rate κ_z is large, the axial motion reaches its equilibrium almost instantaneously relative to the other relevant time scales. If in addition the externally applied voltage is large, the stationary state of the axial motion is close to a highly excited coherent state. This dynamical regime is called the quantum Brownian motion (QBM) limit [14] and is realized when $\lambda=\kappa_z/\omega_{\rm rc}$ becomes large, with $\omega_{\rm rc}$ and $|\beta_z|^2\omega_{\rm rc}/\kappa_z^3$ being held constant [11]. In this limit the density operator ρ of the cyclotron, spin, and axial motion factorizes approximately into $\rho=\rho_z\otimes W+O(\lambda^{-1})$ [14], where ρ_z (W) represents the density operator of the axial motion (of the cyclotron and spin motion), respectively. Thus by tracing out the strongly driven and damped axial electronic motion the master equation

$$\dot{W}=-\frac{i}{\hbar}[\tilde{H},W]+\sum_{j=1}^{2}\left(L_jWL_j^\dagger-\frac{1}{2}L_j^\dagger L_jW-\frac{1}{2}WL_j^\dagger L_j\right)$$
$$-\Gamma[N,[N,W]] \tag{20}$$

is obtained for the reduced density operator of the cyclotron and spin motion [11]. The deterministic part of the reduced dynamics is described by the Hamiltonian

$$\tilde{H}=\hbar\tilde{\Omega}_+a_+^\dagger a_+ +\frac{1}{2}\hbar\tilde{\Omega}_s\sigma_z-\hbar\omega_{\rm rc}\left(\frac{\omega_+}{\omega_z}\right)$$
$$\times(1+a_+^\dagger a_+ +\sigma_z)a_+^\dagger a_+ +\hbar(\beta a_+{}^\dagger e^{-i\omega_p t}+\beta^* a_+ e^{i\omega_p t}) \tag{21}$$

with the modified frequencies $\tilde{\Omega}_+=\Omega_+ +\omega_{\rm rc}\langle n_z\rangle_0$ and $\tilde{\Omega}_s=\Omega_s+g/2\omega_{\rm rc}\langle n_z\rangle_0$. The stationary excitation number $\langle n_z\rangle_0$ of the axial motion in the absence of the relativistic coupling to the other degrees of freedom is given by $\langle n_z\rangle_0=4|\beta_z|^2/\kappa_z^2+\overline{n_z}$.

The dissipative part of the dynamics is characterized by the Lindblad operators L_1 and L_2 of Eq. (14). The stochastic influence of the back action of the axial motion on the cyclotron and spin degrees of freedom is described by the Hermitian Lindblad operator

$$L_\Gamma=\sqrt{2\Gamma}N. \tag{22}$$

This Lindblad operator tends to destroy all quantum coherences between different eigenstates of the cyclotron and spin number operator N of Eq. (12) with rate

$$\Gamma=\frac{\omega_{\rm rc}^2}{\kappa_z/2}\frac{|\beta_z|^2}{(\kappa_z/2)^2}(1+2\overline{n_z})[1+O(\lambda^{-1})]. \tag{23}$$

Thus this Lindblad operator might be interpreted as describing the continuous measurement of the observable N with Γ denoting the mean reduction rate.

In order to establish a relationship between the mean value of the measured out-of-phase current $\langle I_{\rm out}\rangle$ and observables referring to the cyclotron and spin degrees of freedom, one starts from the equation of motion for the mean value $\langle \overline{a_z}\rangle = \langle a_z e^{i\omega_d t}\rangle$ using the Hamiltonian (10) and the Lindblad operators L_3 and L_4, i.e.,

$$\frac{d\langle \overline{a_z}\rangle}{dt} = -i(\Omega_z-\omega_d)\langle \overline{a_z}\rangle - \frac{1}{2}\kappa_z\langle \overline{a_z}\rangle - i\beta_z - i\omega_{\rm rc}\langle N\overline{a_z}\rangle. \tag{24}$$

Factorizing the density operator ρ and setting the axial drive in resonance with the axial frequency, i.e., $\Omega_z=\omega_d$, the relation

$$\langle I_{\rm out}\rangle = -2\sqrt{\frac{\hbar\omega_z}{2L_{\rm ind}}}\frac{{\rm Im}(\beta_z)}{(\kappa_z)^2}\omega_{\rm rc}\langle N\rangle \tag{25}$$

is obtained in the stationary limit, i.e., for $t\gg 1/\kappa_z$. This equation shows that in the QBM limit the measurement of the out-of-phase current $\langle I_{\rm out}\rangle$ is equivalent to measurement of the cyclotron and spin excitation number $\langle N\rangle$ [11].

E. Stochastic simulations of individual quantum measurement processes with the quantum state diffusion model

The master equations (13) and (20) together with Eq. (25) describe the time evolution of a statistical ensemble of continuous measurements performed on an electron in a Penning trap. In order to describe the corresponding time evolution of an individual measurement record of $\langle I_{\rm out}\rangle$ by stochastic simulation, in principle a detailed analysis of the measurement process is required on the basis of the quantum-mechanical measurement postulates. So far such an analysis of the continuous measurement of the current $\langle I_{\rm out}\rangle$, which relies on purely electronic means and does not involve any photon counting process, does not exist and its development is beyond the scope of the present work. Nevertheless, in order to obtain some insight into the time evolution of possible individual measurement records of $\langle I_{\rm out}\rangle$ in the subsequent discussions, the quantum state diffusion (QSD) model of state reduction will be used.

This model of state reduction has been introduced as a general approach to continuous quantum measurement processes in which the time evolution of an individual quantum system, i.e., a single member of a statistical ensemble, is represented explicitly [8,9]. In this respect the QSD model transcends the framework of traditional quantum mechanics and its significance for the quantum-mechanical measurement problem still remains an open question. However, starting from the quantum optical photon counting theory it has been demonstrated, for example, that in heterodyning measurements individual records of photocurrents can be described by stochastic differential equations of the QSD type [15]. Thus despite the lack of any systematic derivation based on first principles, the application of the QSD model in this context might be motivated by the formal analogy between the continuous measurement of $\langle I_{\rm out}\rangle$ and quantum optical heterodyning experiments as mentioned in Sec. II C.

In the QSD model, the quantum state of an individual quantum system is represented by a normalized vector $|\psi\rangle_\xi$ in a Hilbert space, which evolves according to the stochastic differential equation

$$|d\psi\rangle_\xi = -\frac{i}{\hbar}H|\psi\rangle_\xi dt - \frac{1}{2}\sum_j (L_j^\dagger L_j + \langle L_j^\dagger\rangle_\psi\langle L_j\rangle_\psi - 2\langle L_j^\dagger\rangle_\psi L_j)|\psi\rangle_\xi dt + \sum_j (L_j - \langle L_j\rangle_\psi)|\psi\rangle_\xi d\xi_j. \tag{26}$$

Thereby $d\xi_j$ are complex Wiener processes with zero mean values, i.e., $M(d\xi_j)=0$, whose correlations are given by

$$d\xi_j d\xi_k = 0 \quad \text{and} \quad d\xi_j d\xi_k^* = \delta_{ij}dt. \tag{27}$$

The quantities $\langle L_j\rangle_\psi = {}_\xi\langle\psi|L_j|\psi\rangle_\xi$ represent expectation values of environment operators L_j with respect to state $|\psi\rangle_\xi$ and M denotes the mean over the statistical ensemble. The dynamical equation (26) has the property that the time evolution of the density operator $\rho = M(|\psi\rangle_{\xi\xi}\langle\psi|)$ of the associated statistical ensemble is given by a master equation of the form of Eq. (13). For any operator A, the quantum-mechanical mean value is given by $\langle A\rangle = {\rm Tr}(\rho A) = M\langle A\rangle_\psi$. For a more detailed presentation of the QSD model, we refer to Refs. [8,9]. A systematic theoretical description of the continuous Stern-Gerlach effect within the framework of the QSD model has been developed in Ref. [11].

Thus, starting from the master equation (20) for the cyclotron and spin motion, individual quantum measurement processes might be simulated within the framework of the QSD model by interpreting $\langle N\rangle_\psi$ as being proportional to the observed current according to Eq. (25).

III. DYNAMICS OF THE ELECTRONIC SPIN

In this section the influence of the relativistic corrections of Secs. II A and II B on the electronic spin is investigated. Starting from the master equation (20) with the Hamiltonian (21) and the three Lindblad operators of Eqs. (14) and (22), the equation of motion for the expectation value of the axial spin component $\langle\sigma_z\rangle = {\rm Tr}(\rho\sigma_z)$ can be obtained. As σ_z commutes with the Hamiltonian, the three Lindblad operators, and their adjoints, the expectation value $\langle\sigma_z\rangle = s_z$ is a constant of motion, i.e.,

$$\frac{d\langle\sigma_z\rangle}{dt} = 0. \tag{28}$$

This also implies that the associated fluctuations of this spin component are time independent, i.e.,

$$\Sigma^{(2)}(\sigma_z) = {\rm Tr}(\rho\sigma_z^2) - ({\rm Tr}(\rho\sigma_z))^2 = 1 - s_z^2. \tag{29}$$

Thus the relativistic couplings discussed in Secs. II A and II B do not affect the ensemble averaged spin motion. But what happens to the electronic spin in an individual continuous measurement process? In order to answer this question completely, a detailed description of the measurement pro-

cess is required, which is a complicated task beyond the main goal of the present investigation. However, some insight into the mechanism underlying the dynamics of the spin in an individual continuous measurement process can be obtained on the basis of the quantum state diffusion (QSD) model. As discussed in Sec. II E, in this model of state reduction the equation for the evolution of the quantum expectation value of an individual measurement process $\langle\sigma_z\rangle_\psi$ is given by

$$d\langle\sigma_z\rangle_\psi=\sum_{j=1,2,\Gamma}\Delta(\sigma_z,L_j)d\xi_j+\Delta(L_j,\sigma_z)d\xi_j^*. \quad (30)$$

$\Delta(A,B)=\langle A^\dagger B\rangle_\psi-\langle A^\dagger\rangle_\psi\langle B\rangle_\psi$ characterizes the quantum correlations of the operators A and B with respect to the state $|\psi\rangle_\xi$, which is a solution of the QSD equation (26). Equation (30) shows that the electron spin fluctuates along an individual quantum trajectory with zero average drift in agreement with the average evolution of Eq. (28). The spin fluctuations depend on the correlations of σ_z with the environment operators L_j with $j=1,2,\Gamma$. A measure of these fluctuations is given by the average spin autocorrelation

$$M\Delta^{(2)}(\sigma_z)=M\langle\sigma_z^2\rangle_\psi-M(\langle\sigma_z\rangle_\psi^2)=1-M(\langle\sigma_z\rangle_\psi^2), \quad (31)$$

which reflects properties of the QSD model and which cannot be evaluated from the density operator of Eq. (20). In general, $M\Delta^{(2)}(\sigma_z)$ is different from autocorrelations such as $\Sigma^{(2)}(\sigma_z)=M\langle\sigma_z^2\rangle_\psi-(M\langle\sigma_z\rangle_\psi)^2$, which can be evaluated from the density operator. As this spin autocorrelation fulfills the equation

$$M\frac{d\Delta^{(2)}(\sigma_z)}{dt}=-2\sum_j M[|\Delta(\sigma_z,L_j)|^2], \quad (32)$$

it decreases with time until the quantum correlations $\Delta(\sigma_z,L_j)$ between the spin and the Lindblad operators become vanishingly small. The quantum correlations on the right-hand side of Eq. (32) vanish, if the quantum state $|\psi\rangle_\xi$ can be factorized according to $|\psi\rangle_\xi=|\phi\rangle_\xi\otimes|s_z\rangle_\xi$, where $|\phi\rangle_\xi$ and $|s_z\rangle_\xi$ denote a cyclotron state and an eigenstate of σ_z. From Eq. (32) it can be shown that

$$M\frac{d\Delta^{(2)}(\sigma_z)}{dt}\leqslant-\Gamma M[|\Delta^{(2)}(\sigma_z)|^2], \quad (33)$$

which demonstrates that the average spin-autocorrelation decays exponentially within a time of the order of Γ^{-1} or less. Thus according to the QSD model of state reduction, the mean measurement rate Γ represents the minimal rate at which the spin is projected onto an eigenstate of σ_z in an individual measurement process.

Thus the relativistic couplings discussed in Secs. II A and II B do not affect the average spin dynamics. The spin expectation value $\langle\sigma_z\rangle$ is a constant of the motion. However, according to the QSD model these relativistic couplings affect individual quantum trajectories by projecting the spin state onto an eigenstate of σ_z with a rate that is larger or equal to the mean measurement rate Γ of Eq. (22). After the completion of this reduction process, the influence of the electronic spin on the dynamics of the cyclotron motion can be described simply by the replacement $\sigma_z\rightarrow\pm1$ in Eqs. (21) and (22) and its influence on the cyclotron motion becomes trivial. Therefore, in the subsequent discussion of the electronic cyclotron motion it will be assumed that such a spin projection has already taken place.

IV. THE ELECTRONIC CYCLOTRON MOTION

In this section the influence of the back action of the quantum-mechanical measurement process on the electronic cyclotron motion is investigated. In view of the discussion in Sec. III, effects arising from the electronic spin are taken into account by the replacement $\sigma_z\rightarrow\pm1$ in Eqs. (21) and (22). Insight into the dynamics of the cyclotron motion in individual measurement processes is obtained on the basis of the quantum state diffusion model.

Starting from Eq. (21) and performing the transformation $\hat{a}_+=a_+e^{i\omega_p t}$, the electronic cyclotron motion is described by the Hamiltonian

$$\hat{H}=\hbar\Delta\omega\hat{a}_+^\dagger\hat{a}_++\hbar(\beta\hat{a}_+^\dagger+\beta^*\hat{a}_+)+\hbar\chi(\hat{a}_+^\dagger\hat{a}_+)^2. \quad (34)$$

The strength of the anharmonicity due to relativistic effects is characterized by $\chi=-\omega_{rc}\omega_+/\omega_z$. The frequency $\Delta\omega=\tilde{\Omega}_+\chi(1+s_z)-\omega_p$ with $s_z=\pm1$ refers to the detuning between the renormalized cyclotron frequency $\tilde{\Omega}_+$ and the driving frequency ω_p of the planar electric field of Eq. (7). For the sake of simplicity, the driving strength β is assumed to be a real number. The reduced density operator of the electronic cyclotron motion is governed by the master equation (20). Thereby dissipative effects due to radiative damping and thermal fluctuations of the cyclotron motion are described by the Lindblad operators $\hat{L}_1=\sqrt{(\bar{n}+1)\kappa}\hat{a}_+$ and $\hat{L}_2=\sqrt{\bar{n}\kappa}\hat{a}_+^\dagger$. The Lindblad operator $\hat{L}_\Gamma=\sqrt{2\Gamma}\hat{a}_+^\dagger\hat{a}_+$ describes the back action of the continuous measurement process on the cyclotron motion.

In the absence of the quantum measurement process, i.e., for $\Gamma=0$, this model has already been investigated previously [4,16]. This simplified model describes a driven, anharmonic oscillator interacting with a thermal bath. A characteristic feature of this model is the appearance of bistability and hysteresis effects. The main aim of the subsequent discussion is to gain an understanding of the mechanism by which the back action of the quantum-mechanical measurement process on the cyclotron motion influences these hysteresis effects.

It is apparent from the equation of motion for $\langle\hat{a}_+\rangle$, i.e.,

$$\frac{d\langle\hat{a}_+\rangle}{dt}=-i[(\Delta\omega+\chi)\langle\hat{a}_+\rangle+\beta+2\chi\langle\hat{a}_+^\dagger\hat{a}_+^2\rangle]-\frac{1}{2}(\kappa+2\Gamma)\langle\hat{a}_+\rangle, \quad (35)$$

that the measurement process tends to increase dissipation according to the replacement $\kappa\rightarrow\kappa+2\Gamma$. In order to obtain a more detailed understanding of characteristic features of the quantum measurement process, let us first of all neglect all anharmonic effects.

A. Harmonic approximation

Neglecting anharmonic effects, i.e., setting $\chi=0$, simple analytical expressions are available for $\langle\hat{a}_+\rangle(t)$ and $\langle\hat{a}_+^\dagger\hat{a}_+\rangle(t)$. In particular, the stationary values are given by

$$\langle\hat{a}_+\rangle_s=-\beta\frac{\Delta\omega+i(\kappa/2+\Gamma)}{\Delta\omega^2+(\kappa/2+\Gamma)^2} \tag{36}$$

and

$$\langle\hat{a}_+^\dagger\hat{a}_+\rangle_s=\overline{n}+|\langle\hat{a}_+\rangle_s|^2\left(1+\frac{2\Gamma}{\kappa}\right). \tag{37}$$

The time evolution of these quantities is given by

$$\langle\hat{a}_+\rangle(t)=\langle\hat{a}_+\rangle_s+[\langle\hat{a}_+\rangle(t=0)-\langle\hat{a}_+\rangle_s]e^{-i\Delta\omega t}e^{-(\kappa/2+\Gamma)t} \tag{38}$$

and

$$\langle\hat{a}_+^\dagger\hat{a}_+\rangle_t=\langle\hat{a}_+^\dagger\hat{a}_+\rangle_s+(\langle\hat{a}_+^\dagger\hat{a}_+\rangle_{t=0}-\langle\hat{a}_+^\dagger\hat{a}_+\rangle_s)e^{-\kappa t}+2\beta\frac{\mathrm{Im}\{(\langle\hat{a}_+\rangle_{t=0}-\langle\hat{a}_+\rangle_s)(\kappa/2-\Gamma+i\Delta\omega)\}}{\Delta\omega^2+(\kappa/2-\Gamma)^2}e^{-\kappa t}$$
$$-2\beta\frac{\mathrm{Im}\{(\langle\hat{a}_+\rangle_{t=0}-\langle\hat{a}_+\rangle_s)(\kappa/2-\Gamma+i\Delta\omega)e^{-i\Delta\omega t}\}}{\Delta\omega^2+(\kappa/2-\Gamma)^2}e^{-(\kappa/2+\Gamma)t} \tag{39}$$

with Im indicating the imaginary part of a complex number. In the special case $\Gamma=\kappa/2$ the time evolution of Eq. (39) is modified to

$$\langle\hat{a}_+^\dagger\hat{a}_+\rangle_t=\langle\hat{a}_+^\dagger\hat{a}_+\rangle_s+(\langle\hat{a}_+^\dagger\hat{a}_+\rangle_{t=0}-\langle\hat{a}_+^\dagger\hat{a}_+\rangle_s)e^{-\kappa t}$$
$$-2\beta te^{-\kappa t}\,\mathrm{Im}\{\langle\hat{a}_+\rangle_{t=0}-\langle\hat{a}_+\rangle_s\}. \tag{40}$$

These analytical results demonstrate that besides increasing the radiative damping rate κ according to the replacement $\kappa\to\kappa+2\Gamma$, the measurement process may also give rise to some less obvious effects such as an increase of the stationary excitation number $\langle\hat{a}_+^\dagger\hat{a}_+\rangle_s$ or a modification of the exponential decays. The study of this linear model shows that effects arising from the quantum measurement process can be neglected as long as $\Gamma\ll\kappa/2$. However, as soon as the measurement rate Γ exceeds $\kappa/2$, the back action of the measurement process on the cyclotron motion is no longer negligible.

B. Anharmonic effects due to relativistic corrections

In order to investigate the influence of the quantum-mechanical measurement process on the hysteresis effects originating from the anharmonic couplings discussed in Secs. II A and II B, let us consider the QSD equation of motion for the expectation value $\langle\hat{a}_+\rangle_\psi$, namely

$$d\langle\hat{a}_+\rangle_\psi=-i[(\Delta\omega+\chi)\langle\hat{a}_+\rangle_\psi+\beta+2\chi\langle\hat{a}_+^\dagger\hat{a}_+^2\rangle_\psi]dt$$
$$-\frac{1}{2}(\kappa+2\Gamma)\langle\hat{a}_+\rangle_\psi dt+\sqrt{(\overline{n}+1)\kappa}[\Delta(\hat{a}_+^\dagger,\hat{a}_+)d\xi_1$$
$$+\Delta^{(2)}(\hat{a}_+)d\xi_1^*]+\sqrt{\overline{n}\kappa}[d\xi_2+\Delta^{(2)}(\hat{a}_+)d\xi_2$$
$$+\Delta(\hat{a}_+^\dagger,\hat{a}_+)d\xi_2^*]+\sqrt{2\Gamma}[\langle\hat{a}_+\rangle_\psi d\xi_3$$
$$+\Delta(\hat{a}_+^\dagger\hat{a}_+,\hat{a}_+)(d\xi_3+d\xi_3^*)]. \tag{41}$$

The deterministic part of this equation is identical to the ensemble averaged equation of motion (35). The remaining terms describe the fluctuations originating from radiative damping, from thermal noise, and from the back action of the measurement process on the cyclotron motion. In the absence of measurement, i.e., for $\Gamma=0$, this equation has already been investigated previously [4,16]. In particular, it has been shown that dissipation due to radiative damping and thermal noise tends to localize a wave packet in phase space. In the limit of a perfectly localized state, i.e., a coherent state, the nonlinear term factorizes according to $\langle\hat{a}_+^\dagger\hat{a}_+^2\rangle_\psi=|\langle\hat{a}_+\rangle_\psi|^2\langle\hat{a}_+\rangle_\psi$ thus reproducing the classical nonlinearity. On the other hand, according to Eq. (41) the measurement process tends to project the state $|\psi\rangle_\xi$ onto an energy eigenstate of the unperturbed cyclotron motion. In this state $\langle\hat{a}_+\rangle_\psi$, $\Delta(\hat{a}_+^\dagger\hat{a}_+,\hat{a}_+)$, and the nonlinear term $\langle\hat{a}_+^\dagger\hat{a}_+^2\rangle_\psi$ vanish. Thus, intuitively we expect the measurement process to produce a quantum correlation, which might even be able to cancel the nonlinearity and thus to destroy all hysteresis effects. In the limit of highly excited cyclotron states, a simplified description of the measurement-induced influences can be obtained with the help of the semiclassical decorrelation approximation.

1. Semiclassical decorrelation approximation

A simplified description of the cyclotron motion can be obtained in the semiclassical limit of a large driving amplitude β. In this limit, quantum expectation values can be decorrelated according to the relation $\langle\hat{a}_+^\dagger\hat{a}_+\rangle_\psi\to\langle\hat{a}_+^\dagger\rangle_\psi\langle\hat{a}_+\rangle_\psi$. Formally this semiclassical limit is obtained from Eq. (41) by applying the scaling transformation

$$t'=t,\quad \kappa'=\kappa,\quad \Gamma'=\Gamma,\quad \Delta\omega'=\Delta\omega,\quad \beta'=\mu\beta,$$
$$\chi'=\frac{1}{\mu^2}\chi,\ \text{and}\ \overline{n'}=\mu^2\overline{n} \tag{42}$$

with the scaling factor $\mu\to\infty$. Scaling transformations of this type have already been discussed previously in connec-

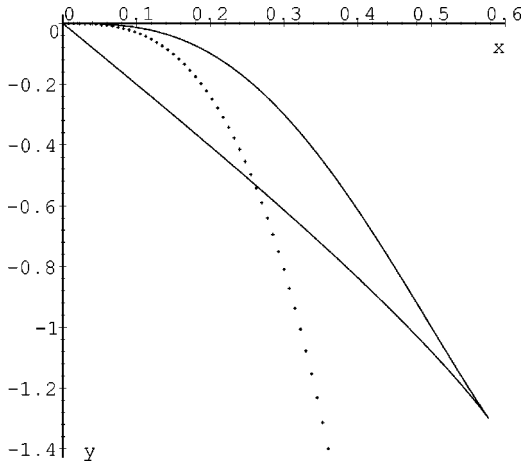

FIG. 1. The border of the bistable domain (full curve) is shown and the location of the system for different values of the measurement rate Γ (dotted curve) with the parameter choice $a=\Delta\omega^3/\beta^2\chi=-30.0$.

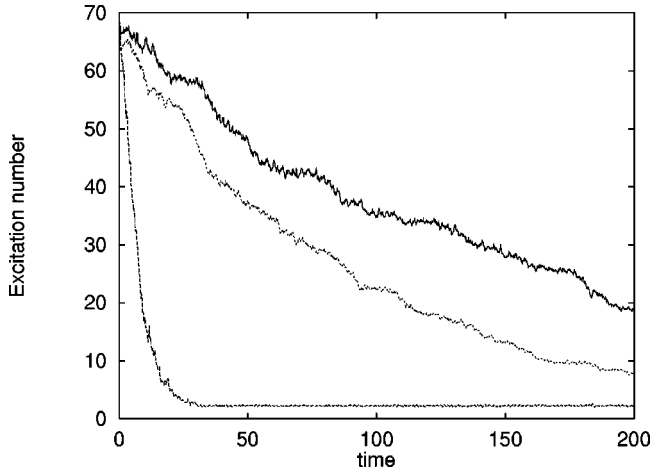

FIG. 2. Time evolution, in arbitrary units, of the ensemble average excitation number using 100 trajectories. The parameters used are $\kappa=1.5$, $\beta=-7.0$, $\bar{n}=0$, $\chi=0.04$, and $\Delta\omega=-5.0$. The initial state is a coherent state centered at a metastable position. The upper curve is for $\Gamma=0$, the lower for $\Gamma=0.1$, and the middle one for $\Gamma=0.01$.

tion with the quantum-classical transition in systems whose classical dynamics are chaotic [17]. Applying this scaling transformation to the QSD equation of motion (41) yields

$$d\alpha=-i(\Delta\omega\alpha+\beta+2\chi|\alpha|^2\alpha)dt-\frac{1}{2}(\kappa+2\Gamma)\alpha dt + \sqrt{\bar{n}\kappa}d\xi_2+\sqrt{2\Gamma}\alpha d\xi_3 \tag{43}$$

with $\alpha=\langle\hat{a}_+\rangle_\psi/\mu$. The semiclassical QSD equation (43) is invariant under the scaling transformation (42) and in the absence of measurement, i.e., for $\Gamma=0$, it reduces to the classical stochastic differential equation for a driven anharmonic oscillator interacting with a thermal bath. Equation (43) contains two noise terms. The first one proportional to $\sqrt{\bar{n}\kappa}$ represents thermal fluctuations while the second one proportional to $\sqrt{2\Gamma}$ is a homogeneous noise induced by the quantum measurement process. Both the thermal and the measurement-induced fluctuations transform the stable equilibrium points, which correspond to the stationary solutions of the deterministic part of Eq. (43), into metastable equilibria. In particular, the measurement process can hide bistability by inducing spontaneous transitions between both metastable equilibrium points. Alternatively, the measurement process can also suppress bistability by displacing equilibrium points out of the bistable domain. This latter point is illustrated in Fig. 1. Each point of Fig. 1 represents a system described by the semiclassical Eq. (43) in the absence of noise, i.e., for $d\xi_2=d\xi_3=0$. The location (x,y) of the system is specified by its parameters where $x=(\kappa/2+\Gamma)/\Delta\omega$ and $y=(\kappa/2+\Gamma)^3/\beta^2\chi$. Bistable behavior is only possible for points located inside the full curve [16]. If, starting from an arbitrary point, we keep all parameters fixed and vary the measurement rate Γ, the point will follow a cubic curve of the form $y=ax^3$ with $a=\Delta\omega^3/\beta^2\chi$. The dots in Fig. 1 represent locations of the system for different values of the measurement rate Γ. The trajectory formed by these points demonstrates that with increasing measurement rate Γ, systems that are bistable in the absence of measurement, i.e., for $\Gamma=0$, eventually become monostable as soon as they cross the border line (full curve). In this latter case all associated hysteresis effects are destroyed.

2. Bistability and measurement-induced fluctuations

Returning to the full QSD equations, we investigate the influence of thermal and measurement-induced fluctuations on bistability in Fig. 2, where the time evolution of the average excitation number $M\langle\hat{a}_+^\dagger\hat{a}_+\rangle_\psi$ is depicted for different values of the measurement rate Γ. The parameters in Fig. 2 are chosen so that in the absence of quantum measurement, i.e., for $\Gamma=0$, the system starts in the bistable domain. The initial state is assumed to be a coherent state centered at one of the two possible metastable equilibrium points. Two different values of the measurement rate have been used to compute the time evolution, which is compared with the time evolution in the absence of measurement. For $\Gamma=0$ the effective decay time of the excitation number is much larger than the radiative damping time $1/\kappa$. This reflects the fact that, in the absence of measurement in the bistable regime, the noise-induced transition time between the two possible metastable states is usually much larger than the inverse characteristic radiative damping time $1/\kappa$ [16]. This transition time depends mainly on the magnitude of the thermal fluctuations. With increasing measurement rate Γ the effective decay time of the excitation number decreases rapidly and finally approaches the radiative damping time $1/\kappa$ in the limit when all effects arising from the nonlinear term $\langle\hat{a}_+^\dagger\hat{a}_+^2\rangle_\psi$ have become insignificant. This demonstrates the profound influence of the quantum measurement process on bistability. The quantum measurement process tends to project the quantum state of the electronic cyclotron motion onto an energy eigenstate that is delocalized spatially and for which the nonlinearity of Eq. (41) vanishes. This removal of the nonlinearity leads to a suppression of bistability, which is exemplified by the rapid change of the effective decay time in Fig. 2.

In Fig. 3, numerical simulations of individual experiments for measuring hysteresis effects are presented. It is assumed

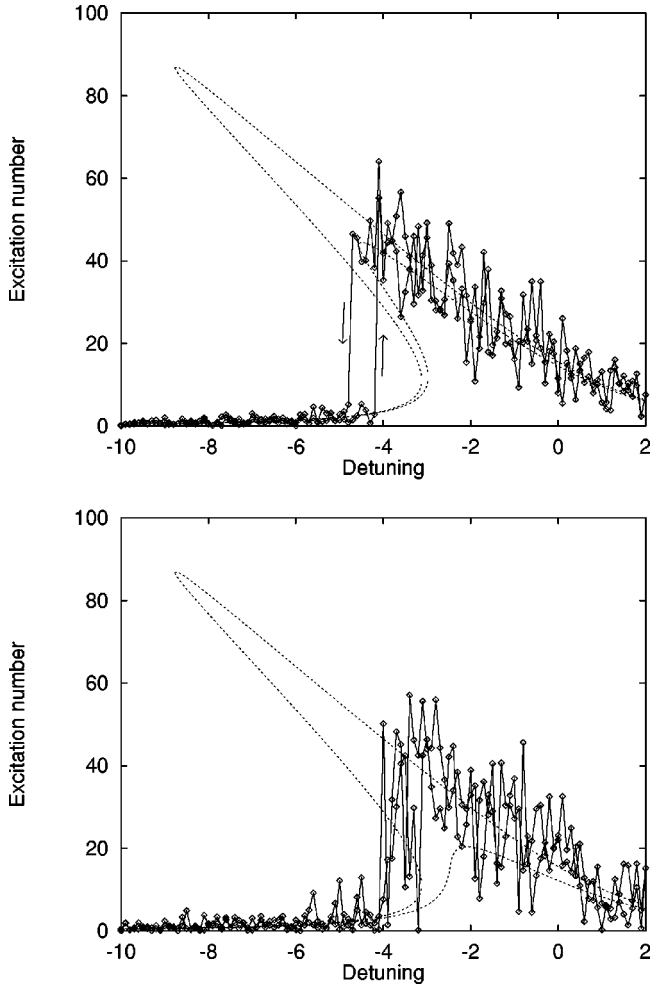

FIG. 3. Numerical simulations of hysteresis experiments, in arbitrary units, using the QSD model with parameters $\kappa=1.5$, $\beta=-7.0$, $\overline{n}=0$, $\chi=0.05$ and for two different measurement rates (a) $\Gamma=0.3$, (b) $\Gamma=0.8$. The detuning step is 0.1 and the measurement delay time is $t_m=50$. The dashed curves represent the classical steady-state excitation numbers with $\Gamma=0$ (curve extending to the far left) and (a) $\Gamma=0.3$, (b) $\Gamma=0.8$.

that the dynamics of a single electron is measured continuously in cases in which its corresponding classical motion is bistable in the absence of measurement. The driving frequency ω_p of the external electronic field is assumed to be varied step by step from low to high frequencies and reversed, thus spanning twice the classically bistable domain. For each value of the driving frequency ω_p it is assumed that the experimenter waits a time t_m, i.e., the measurement delay, and records the excitation number $\langle a_+^\dagger a_+ \rangle_\psi$ before changing ω_p again. The measurement delay is assumed to be much larger than the characteristic radiative damping time $1/\kappa$. Thus the driving frequency is swept adiabatically with respect to the radiative damping time $1/\kappa$.

According to the QSD model of state reduction, such an experiment is described theoretically by curves like the ones shown in Fig. 3. The measured excitation number $\langle a_+^\dagger a_+ \rangle_\psi$ fluctuates around one of the two classical steady states for a while and then jumps to the other value. The two jumps [indicated by vertical arrows in Fig. 3(a)] occurring when the driving frequency is ramped from low to high frequencies and reversed allows one to define a detuning width $\Delta\Omega$ as the size of the bistable region in an individual realization. This detuning width $\Delta\Omega$ is a random variable and is different for each realization of an experiment.

As has already been discussed previously [16], in general the statistical properties of this detuning width $\Delta\Omega$ depend on the ratio between the measurement delay time t_m and the mean stochastic transition time τ between the classical steady states. In the absence of quantum measurement, i.e., for $\Gamma=0$, this latter time is typically much larger than the radiative damping time $1/\kappa$ and depends on the magnitude of the thermal fluctuations [16]. Two limiting cases can be distinguished. (i) If the measurement delay is small relative to the stochastic transition time, i.e., $\tau \gg t_m$, then in general $\Delta\Omega$ has a finite value thus exhibiting bistability. (ii) At the opposite extreme, i.e., for $\tau \ll t_m$, the detuning width $\Delta\Omega$ is equal to zero, thus indicating the disappearance of hysteresis effects.

The back action of the continuous measurement process on the electronic cyclotron motion tends to project the state onto a spatially delocalized energy eigenstate. Therefore it is expected that with increasing measurement rate Γ the mean stochastic transition time τ decreases, thus eventually leading to a measurement-induced disappearance of hysteresis effects. This behavior is exemplified by the individual realizations depicted in Figs. 3(a) and 3(b). In Fig. 3(a) the mean measurement rate Γ is of the order of the radiative damping rate κ. As a consequence, the detuning width is much smaller than the classically expected value in the absence of measurement (dashed curve extending to the far left). However, hysteresis effects are still apparent. In Fig. 3(b) the measurement rate Γ is already so large that all hysteresis effects have disappeared even in the classical limit (dashed curve) due to the fast stochastic transitions between the classical steady states. As a consequence these rapid stochastic transitions give rise to fluctuations of the measured excitation number $\langle a_+^\dagger a_+ \rangle_\psi$ that are much larger than in the case depicted in Fig. 3(a).

V. CONCLUSION

A detailed quantum-mechanical description of the relativistic dynamics of a single electron in a Penning trap has been developed in which interaction with the environment has been taken into account. To this end we have retained the radiative damping of the cyclotron motion and dissipative effects of the axial motion originating from the readout resistor. The relativistic effects lead to nonlinear couplings between the electronic cyclotron, spin, and axial motion. Thus the electronic cyclotron and spin motion can be monitored continuously by measuring the charge-induced currents of the axial motion.

A master equation has been derived that describes the dynamics of a statistical ensemble of continuous quantum measurements performed on an electron in the Penning trap. The electronic axial motion, which might be considered as part of the measurement apparatus, has been eliminated adiabatically in the limit of rapid axial dissipation, i.e., in the quantum Brownian motion limit. In this limit the measurement apparatus is sensitive to the electronic cyclotron and spin quantum number and the mean rate of reduction Γ can

be varied over many orders of magnitude by altering the external driving of the axial motion, similar to the harmonic case presented earlier in Ref. [11]. It has been shown that this measurement process tends to project the electronic spin along the axial direction. After the completion of this projection process, the relativistic effects do not give rise to any further spin flips.

It has been demonstrated that the continuous quantum measurement process has a profound influence on the cyclotron motion and its bistable behavior. The QSD model provides an intuitively appealing description of the competition between dissipative effects originating from radiative damping of the cyclotron motion and thermal noise, which tend to localize the cyclotron state into a coherent state, and the measurement-induced effects, which tend to project the cyclotron state into a spatially delocalized energy eigenstate of the unperturbed cyclotron motion. The relative strength of these two competing stochastic processes depends on the ratio between the measurement rate Γ and the radiative damping rate κ of the cyclotron motion.

ACKNOWLEDGMENTS

We would like to thank Gerald Gabrielse, Nicolas Gisin, Daphna Henzer, Ian Percival, and Rüdiger Schack for stimulating discussions. This work was supported by the EU under its Human Capital and Mobility Programme and the Deutsche Forschungsgemeinschaft within the Schwerpunktprogramm ''Zeitabhängige Phänomene in Quantensystemen der Physik und Chemie.''

[1] L. S. Brown and G. Gabrielse, Rev. Mod. Phys. **58**, 233 (1986).
[2] G. Gabrielse, H. Dehmelt, and W. Kells, Phys. Rev. Lett. **54**, 537 (1985).
[3] C. H. Tseng and G. Gabrielse, Appl. Phys. B: Lasers Opt. **60**, 95 (1995).
[4] D. Enzer and G. Gabrielse, Phys. Rev. Lett. **78**, 1211 (1997).
[5] A. E. Kaplan, Phys. Rev. Lett. **48**, 138 (1982).
[6] I. Marzoli and P. Tombesi, Europhys. Lett. **24**, 515 (1993).
[7] P. Lerner and P. Tombesi, Phys. Rev. A **47**, 4436 (1993).
[8] N. Gisin and I. C. Percival, J. Phys. A **25**, 5677 (1992).
[9] I. C. Percival, *Quantum State Diffusion* (Cambridge University Press, Cambridge, 1998).
[10] J. D. Bjorken and S. D. Drell, *Relativistic Quantum Mechanics* (McGraw-Hill, New York, 1964).
[11] T. Steimle and G. Alber, Phys. Rev. A **53**, 1982 (1996).
[12] T. Steimle, Ph.D. thesis, University of Freiburg, Freiburg, Germany, 1995.
[13] W. Louisell, *Quantum Statistical Properties of Radiation* (John Wiley and Sons, New York, 1973).
[14] C. W. Gardiner, *Quantum Noise* (Springer, Berlin, 1991).
[15] H. Carmichael, *An Open Systems Approach to Quantum Optics*, Lecture Notes in Physics Vol. 18 (Springer, Berlin, 1993).
[16] M. Rigo, G. Alber, F. Mota-Furtado, and P. F. O'Mahony, Phys. Rev. A **55**, 1665 (1997).
[17] M. Rigo, F. Mota-Furtado, and P. F. O'Mahony, J. Phys. A **30**, 7557 (1997).